Maximum size of bubbles during nucleate boiling in an electric field

K. J. Cheng and J. B. Chaddock*

By taking account of the electric field effects on the shape of bubbles, Fritz's analysis on maximum bubble volume during boiling was extended to the boiling process in the presence of a uniform electric field. It was found that the maximum bubble volume decreases with increase in electric field strength and the dielectric constant of the boiling liquid. The decrease of bubble departure size with increase in electric field strength was confirmed by experimental observations.

Keywords: *bubble departure size, nucleate boiling, electric field effects*

Introduction

It has been well documented that an electric field can enhance the boiling process significantly[1-4]. The major observed effects of an electric field on boiling include (i) increase of the maximum heat flux, (ii) suppression of film boiling, and (iii) decrease of bubble departure size. Much effort has been made to explain this change in boiling behaviour in the presence of an electric field, with focus being on the field-coupled Rayleigh-Taylor instability, the dielectrophoresis effect, and the condenser effect. Lovenguth[5], Johnson[6], and Berghmans[7] have studied the electric field effects on the maximum heat flux and film boiling using the field-coupled Rayleigh–Taylor instability analysis. Pohl[8] has studied the dielectrophoresis effect on a boiling liquid in a nonuniform electric field, which induces motion of vapour bubbles towards the region of lower field strength. Markels and Durfee[2,3] have suggested that a condenser effect (coulomb attraction between plates of a condenser) causes an increased wettting of the heating surface by the boiling liquid.

The studies cited above have devoted little attention to the change in pertinent thermophysical properties of the fluid, ie surface tension, contact angle and thermal conductivity. The presence of an electric field has been observed to affect the magnitude of these properties as well as the basic mechanisms of the boiling process, which include bubble nucleation, growth and departure. It is known from the theory of electrocapillarity that the surface tension between two media decreases in the presence of charges at the boundary[9-11]. According to the hydrodynamic model of boiling instability, a decreases of surface tension should cause a decrease of maximum and minimum heat fluxes. Increase in thermal conductivity of dielectric fluid when subjected to an electric field has been observed[12,13], and a theoretical explanation of this phenomenon probably requires a study of the electric field effect on phonon propagation. Effects of an electric field on bubble nucleation and bubble growth have been reported elsewhere by us[14,15].

In this paper, we examine the effect of an electric field on bubble departure size. Our study is based on Fritz's analysis[16] on the maximum volume attainable by a bubble with a given contact angle during its growth. The effect of the electric field is to elongate the bubble. As a result, the maximum volume decreases with increase in the strength of the electric field and the dielectric constant of the boiling liquid. The decrease of bubble departure size by the electric field has been observed by numerous investigators, including Choi[17], Lovenguth[5], and Markels and Durfee[2]. However, no attempt to calculate the bubble departure size in the presence of an electric field has been reported yet.

Maximum bubble size in the absence of an electric field

The classical study on bubble departure size during nucleate boiling was done by Fritz. The essence of his analysis is the application of the Laplace formula

$$P_v - P_l = \sigma\left(\frac{1}{R_1} + \frac{1}{R_2}\right)$$

to the interface of the vapour bubble and the liquid. Herein P_v and P_l are the vapour and liquid pressures, respectively, σ is the surface tension coefficient, and R_1 and R_2 are the principal radii of curvature of the surface. The geometry of the bubble is as shown in Fig 1. Substituting the curvature formulas for R_1 and R_2, and using

$$P_v - P_l = 2\frac{\sigma}{R} - \rho g Y$$

where R is the radius of curvature at the tip of the bubble and $\rho \equiv \rho_l - \rho_v$ is the difference in densities between the

* Department of Mechanical Engineering and Materials Science, Duke University, Durham, NC 27706, USA

0142–727X/86/040278–05$3.00

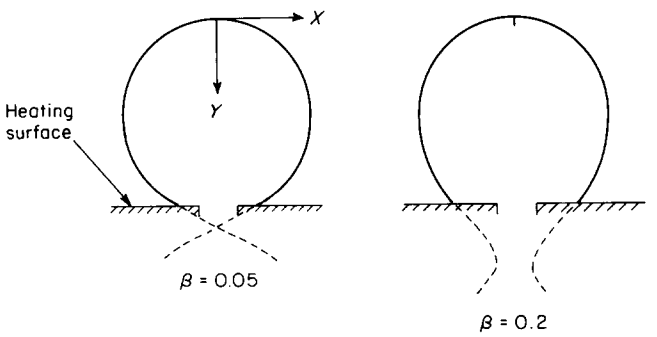

Fig 1 Bubble profiles without electric field

liquid and the vapour, the Laplace formula becomes

$$\frac{\dfrac{d^2Y}{dX^2}}{\left\{1+\left(\dfrac{dY}{dX}\right)^2\right\}^{3/2}}+\frac{\dfrac{1}{X}\dfrac{dY}{dX}}{\left\{1+\left(\dfrac{dY}{dX}\right)^2\right\}^{1/2}}=\frac{2}{R}-\frac{\rho g Y}{\sigma} \tag{1}$$

Eq (1) determines the profile of the bubble. Detachment occurs when the bubble volume above the plane of contact reaches a maximum. Using Eq (1), Fritz was able to derive a relationship between the maximum bubble volume V_m, and the contact angle ϕ (Fig 4 of Ref 16) which can be expressed approximately as

$$V_m^{1/3}\left(\frac{\rho g}{\sigma}\right)^{1/2}=0.01667\phi \tag{2}$$

where ϕ is measured in degrees. Defining an equivalent departure radius R_d such that $V_m=4/3\pi(R_d)^3$, we obtain the well-known formula

$$R_d=0.0103\phi\left(\frac{\sigma}{\rho g}\right)^{1/2} \tag{3}$$

(We should like to point out here that many textbooks and other items of literature have mistakenly attributed the departure radius/diameter formula, Eq (3), to Fritz. Fritz did not derive that formula. Fritz's original result was presented graphically as a relation between $V_m^{1/3}(\rho g/\sigma)^{1/2}$ and ϕ. His graph was latter fitted into Eq (2) by some subsequent authors. Eq (2) wss then eventually changed into Eq (3) in the literature by some other authors. Furthermore, Fritz's solution is a numerical one, not empirical as suggested by many textbooks.)

Before proceeding to the calculation of bubble volume in an electric field, we shall outline a simple numerical procedure that can be used to generate Fritz's result. The calculation of bubble volume in an electric field will be a simple extension of this procedure.

We first introduce the dimensionless coordinates $x=X/R$, $y=Y/R$, and the bubble scale factor $\beta=\rho g/\sigma R^2$. It is also more convenient to use y as the independent variable and write the curvature formulas in terms of dx/dy and d^2x/dy^2 rather than dy/dx *and* d^2y/dx^2 as in Eq (1). Eq (1) thus becomes

$$-\frac{\dfrac{d^2x}{dy^2}}{\left\{1+\left(\dfrac{dx}{dy}\right)^2\right\}^{3/2}}+\frac{1}{x\left\{1+\left(\dfrac{dx}{dy}\right)^2\right\}^{1/2}}=2-\beta y \tag{4}$$

Eq (1) is inconvenient to solve numerically because y is a multiple-valued function of x, and also because dy/dx is infinite in the middle of the profile. However, these problems can be avoided by using Eq (4) since x is a single-valued function of y, and dx/dy is finite except at the origin. Eq (4) can be easily solved numerically using any standard subroutine for solving ordinary differential equations. In view of the singularity of dx/dy at the origin, we start the numerical solution at a point slightly off the origin. This was arbitrarily chosen as $x=0.02$. Since the profile is almost spherical at the tip, the corresponding values of y and dx/dy can be estimated using the equation of the circle: $x^2+(y-1)^2=1$. Thus our initial conditions are: $x=0.02$, $y=1-(1-x^2)^{1/2}$, and $dx/dy=(1-y)/x$. Solution of Eq (4) gives the bubble profile for a given value of β. Some of the profiles generated are shown in Fig 1. It can be seen that the effect of gravity ($\beta\neq 0$) is to cause the bubble to assume a profile that has a neck at the bottom.

Once the profile is determined, the volumes from the bubble tip down to horizontal planes with various contact angles can be calculated. We shall denote this quantity in dimensional form by V, and in dimensionless form by $v=V/R^3$. Repeating this calculation for many values of the bubble scale factor β generates a table that displays the dependence of v on β and ϕ (Table 1). It can be seen from the table that for a given ϕ, the volume reaches a maximum at a certain value of β. Hereafter, this maximum volume and the corresponding value of the

Notation

e	Eccentricity
E	Electric field strength
g	Gravitational acceleration
P_v	Hydrostatic pressure in bubble
P_l	Hydrostatic pressure in liquid
r	Equivalent radius of spheroidal bubble
R	Radius of curvature at bubble tip
R_1, R_2	Principal radii of curvature of bubble surface
R_d	Equivalent bubble radius at departure
v	Dimensionless bubble volume $\equiv V/R^3$
v_m	Dimensionless maximum bubble volume
V	Dimensional bubble volume
V_m	Dimensional maximum bubble volume
x	Dimensionless x coordinate $\equiv x/R$
X	Dimensional X coordinate
y	Dimensionless y coordinate $\equiv y/R$
Y	Dimensional Y coordinate
α	Aspect ratio of spheroidal bubble; elongation factor of nonspheroidal bubble
β	Bubble scale factor $\equiv \rho g/\sigma R^2$
β_m	Maximum bubble scale factor
ε_0	Permittivity of free space $= 8.854\times 10^{-12}$ C^2 N^{-1} m^{-2} in SI units
ε_l	Dielectric constant of liquid
ε_v	Dielectric constant of vapour
ϕ	Contact angle, degrees
ρ_v	Vapour density
ρ_l	Liquid density
ρ	$\rho_l-\rho_v$
σ	Surface tension coefficient

Table 1 Dimensionless bubble volume v as a function of contact angle ϕ and bubble scale factor β at $\alpha=1.0$

β \ ϕ	25°	35°	45°
0.06	4.448	4.376	4.218
0.07	–	4.429	4.269
0.09	–	4.542	4.377
0.11	–	4.668	4.491
0.12	–	4.739	4.554
0.13	–	–	4.619

A dash indicates that contact angle equal to or less than that value of ϕ does not exist on the bubble profile

bubble scale factor will be denoted by v_m and β_m, respectively. When the bubble scale factor increases beyond β_m, contact angles smaller than the given ϕ cannot exist on the profile. The value of v_m is, of course, the departure size corresponding to that particular contact angle. By generating profiles for enough values of β, the maximum volume for each value of ϕ can be determined to any desired accuracy. Figs 2(a) and 2(b) show the dependences of $v_m^{1/3}\beta_m^{1/2}(=V_m^{1/3}(\rho g/\sigma)^{1/2})$ and $\beta_m^{1/2}(=(\rho g/\sigma)^{1/2}R)$ on ϕ. The $V_m^{1/3}\beta_m^{1/2}$ versus ϕ plot at zero electric field ($E=0$) is almost a straight line. This is essentially the same as Fig 4 in Fritz's paper from which Eqs (2) and (3) given above are obtained.

Maximum bubble size in an electric field

It can be shown theoretically, and has been well documented experimentally, that spherical bubbles and drops are elongated to approximately prolate spheroids by a uniform electric field, the elongation being along the direction of the field[18-20]. A simple method for calculating the elongation of spheroidal bubbles in an electric field by considering the variation of free energy has been presented by the authors in an earlier paper[21]. Here we would merely give the equation that determines the elongation of the speroidal bubble as

$$\frac{\partial}{\partial\alpha}\left(\alpha^{-2/3}+\alpha^{1/3}\frac{\sin^{-1}e}{e}\right)-\frac{\varepsilon_0 E^2 r}{3\sigma}\frac{\partial H}{\partial\alpha}=0 \qquad (5)$$

where

$$H=\frac{(\varepsilon_v-\varepsilon_l)\varepsilon_l}{(1-n)\varepsilon_l+n\varepsilon_v}$$

$$n=\frac{1-e^2}{2e^3}\left(\ln\frac{1+e}{1+e}-2e\right)$$

E is the electric field strength, e is the eccentricity, $\alpha=(1-e^2)^{-1/2}$ is the aspect ratio (major radius divided by minor radius), ε_0 is the permittivity of free space, ε_v and ε_l are the dielectric permittivities of the vapour bubble and liquid, respectively, and r is equivalent bubble radius.

If $\varepsilon_l \gg \varepsilon_v$ (eg for water and most other polar liquids), then α is a function only of the parameter $\varepsilon_0\varepsilon_l E^2 r/\sigma$. This is shown in Fig 3(a). For nonpolar liquids where ε_l is small (eg Freons, where $6>\varepsilon_l>2$), the value of α depends on the individual values of $\varepsilon_0 E^2 r/\sigma$ and ε_l. Fig 3(b) shows α as a function of $\varepsilon_0 E2r/\sigma$ for $\varepsilon_l=2.4$ (Freon 113) and $\varepsilon_l=5.65$ (Freon 21).

Eq (5) was derived for bubbles with spheroidal profiles when the effect of gravity is neglected. We now assume that the bubbles with profiles as determined in the previous section are also elongated by the electric field according to Eq (5), where the r in Eq (5) is to be identified as the R defined in the previous section. The coordinates of the bubble profile in the presence of an electric field $(\tilde{x},\tilde{y})$ are thus related to the zero-field values (x,y) by

$$\tilde{x}=\alpha^{-1/3}x \qquad \tilde{y}=\alpha^{2/3}y \qquad (6)$$

Notice the bubble volume (proportional to x^2y) is invariant under this transformation. When $\beta=0$ (which gives a closed spherical bubble at zero electric field strength), Eq (6) is exact. For small values of β (when the bubble profiles do not deviate too far from the spherical shape at zero electric field strength), Eq (6) can be expected to hold approximately. In the analysis that follows, we shall thus confine our analysis to the case where β is small. Some profiles of bubbles elongated by a uniform electric field are shown in Fig 4.

Once the bubble profile is known, the same procedure outlined in the previous section can be applied to obtain the dependence of $v_m^{1/3}\beta_m^{1/2}$ and $\beta_m^{1/2}$ on ϕ for

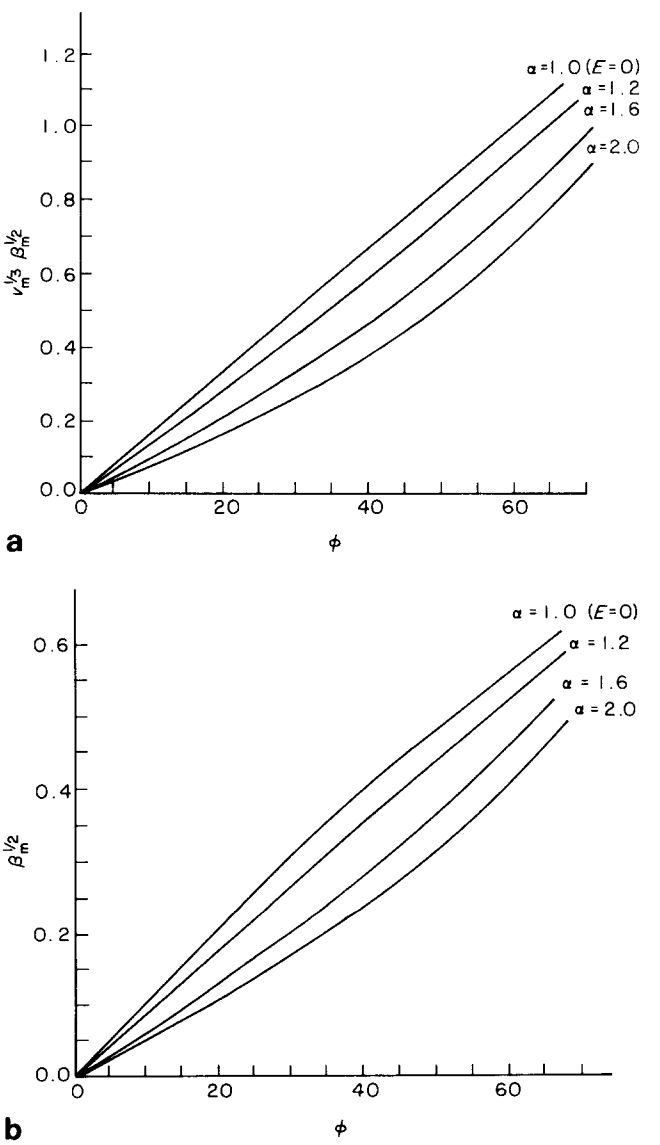

Fig 2 (*a*) $v_m^{1/3}\beta_m^{1/2}$ *as a function of* ϕ. (*b*) $\beta_m^{1/2}$ *as a function of* ϕ

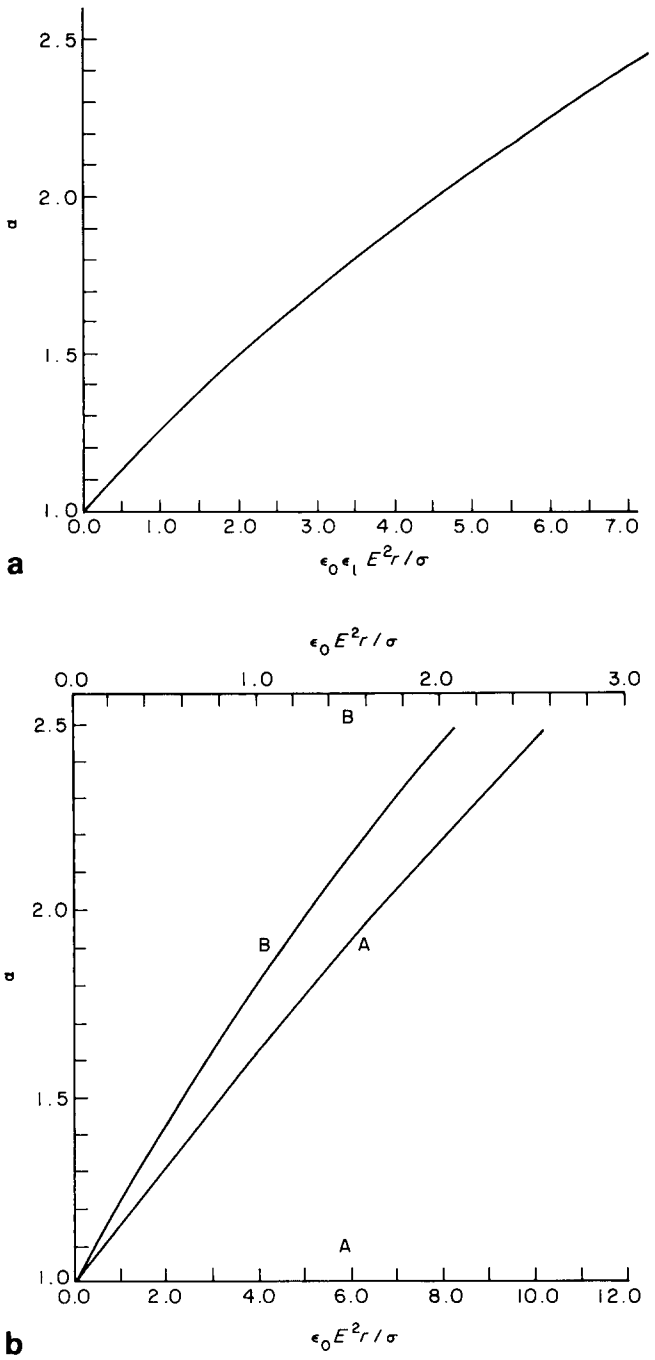

Fig 3 (a) α as a function of $\varepsilon_0\varepsilon_l E^2 r/\sigma$ *for* $\varepsilon_l \gg \varepsilon_v$, $\varepsilon_v = 1.0$. *(b) α as a function of* $\varepsilon_0 E^2 r/\sigma$: *A* $\varepsilon_l = 2.4$, $\varepsilon_v = 1.0$; *B* $\varepsilon_l = 5.65$; $\varepsilon_v = 1.0$

various value of α (Figs 2(a) and 2(b)). In doing so, we have ignored the possible effect of the electric field on σ and ϕ.

Fig 2(a), together with Figs 3(a) or 3(b), determine the bubble departure size for given values of ε_l, E^2, σ, ρ, and ϕ. However, Figs 3(a) and 3(b) are inconvient to use because their abscissa contains an unknown quantity, R, which increases as the bubble grows. To present the results in a more useful form, we use Figs 2(b), 3(a) and 3(b) to eliminate R, and then plot $v_m^{1/3}\beta_m^{1/2}$ as a function of $(\varepsilon_0 E^2/\sigma)(\sigma/\rho g)^{1/2}$ for various contact angles as in Figs 5(a), 5(b) and 5(c). These are essentially plots of dimensionless bubble departure size versus the dimensionless electric field strength.

Comparison of analysis with experimental data

In Fig 5(b), we have also marked the experimental values of the dimensionless bubble departure size obtained by Lovenguth (p 70 of Ref 5) using Freon 21 ($\varepsilon_l = 5.65$) at various electric field strengths. Direct comparison of Lovenguth's experimental data with our analysis is difficult because the contact angle, which is an essential part of Fritz's model of bubble departure, is not given in Lovenguth's work. The static contact angle of Freon 113 has been measured to be about 1°–4° by Bergles[22], and the static contact angle of Freon 21 is expected to be about the same. However, as pointed out by Han and Griffith[23], Fritz's departure criterion ought to be used with the dynamic rather than the static contact angle. In general, the dynamic contact angles are larger than the static values.

Comparison of our analysis with Lovenguth's data is further complicated by the fact that in Lovenguth's experiments, the electric field is not uniform by cylindrical. This cylindrical field geometry introduces an extra dielectrophoresis force which tends to move the bubble away from the heating surface and should result in departure size smaller than that predicted by the present analysis. Despite this, his data seem to agree with our anaylsis in order of magnitude.

Discussion

It is obvious from Figs 2(a), 3(a) and 3(b) that as the dielectric constant of the liquid and the electric field strength increase, the bubble departure size decreases. Moreover, the electric field strength appears only as E^2 in the analysis. In other words, the polarity of the electric field is immaterial in our modelling.

It has been recognized that an electric field can provide a versatile means to augment many industrial boiling heat transfer processes. This paper presents a basic study on how a uniform electric field reduces the bubble departure size during the nucleate boiling process. Our results can be used as a guideline in the boiling processes where it is desired to control the bubble departure size by means of an external electric field.

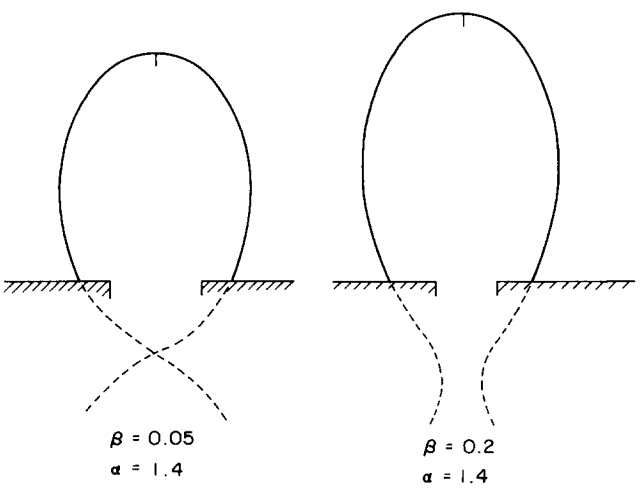

Fig 4 Bubble profiles in the presence of an electric field

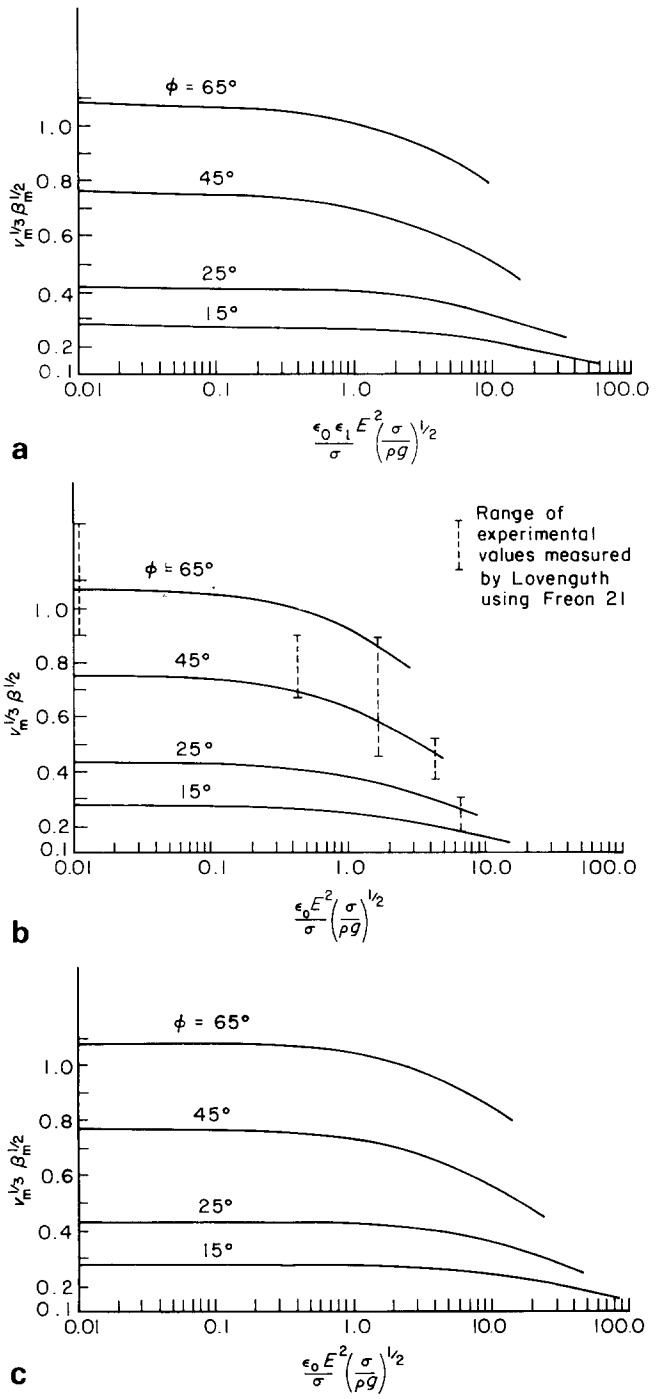

Fig 5 (*a*) $v_m^{1/3}\beta_m^{1/2}$ *as a function of* $\varepsilon_0\varepsilon_l E^2/\sigma\,(\sigma/\rho g)^{1/2}$ *for* $\varepsilon_l \gg \varepsilon_v$, $\varepsilon_v = 1.0$. (*b*) $v_m^{1/3}\beta_m^{1/2}$ *as a function of* $\varepsilon_0 E^2/\sigma\,(\sigma/\rho g)^{1/2}$ *for* $\varepsilon_l = 5.65$, $\varepsilon_v = 1.0$. (*c*) $v_m^{1/3}\beta_m^{1/2}$ *as a function of* $\varepsilon_0 E^2/\sigma\,(\sigma/\rho g)^{1/2}$ *for* $\varepsilon_l = 2.4$, $\varepsilon_v = 1.0$

Conclusions

(1) Fritz's analysis on maximum bubble size was extended to the boiling process in the presence of a uniform electric field by taking account of the electric field effects on the bubble shape.
(2) It was found that the bubble departure size decreases as the electric field strength and dielectric constant of the liquid increase.
(3) Some plots are given showing the relationships between the electrical parameters (ε_l and E) and the bubble deformation and departure size.

Acknowledgement

We are grateful to Professor A. E. Bergles of Iowa State University for some valuable comments.

References

1. **Jones T. B.** Electrohydrodynamically enhanced heat transfer in liquids—a review in *Advances in Heat Transfer*, *1978*, **14**, *107–148*
2. **Markels M. and Durfee R. L.** The effect of applied voltage on boiling heat transfer. *AIChE J.*, *1964*, **10**, *106–110*
3. **Markels M. and Durfee R. L.** Studies of boiling heat transfer with electrical fields. *AIChE J.*, *1965*, **11**, *716–723*
4. **Zhorzholiani A. G. and Shekriladze I. G.** Study of the effect of an electrostatic-field on heat transfer with boiling dielectric fluids. *Heat Transfer—Soviet Research*, *1972*, **4**, *81–98*
5. **Lovenguth R. F.** Boiling heat transfer in the presence of electric fields. *PhD Dissertation, Dept. Chem. Eng., Newark College of Engineering, 1968*
6. **Johnson R. L.** Effect of an electric field on boiling heat transfer. *AIAA J.*, *1968*, **6**(*8*), *1456–1460*
7. **Berghmans J.** Electrostatic fields and the maximum heat flux. *Int. J. Heat Mass Transfer*, *1976*, **10**, *791–797*
8. **Pohl H. A.** Some effects of nonuniform fields on dielectrics. *J. Appl. Phys.*, *1958*, **29**(*8*), *1182–1188*
9. **Kovagchuk E. U. and Scekatogina S. A.** Electrical contributions to the surface tension coefficient of polar liquids. *Ukranian Phys. J.*, *1982*, **27**(*10*), *1528–1534* (*in Russian*)
10. **Landau L. D. and Lifshitz E. M.** *Electrodynamics of Continuous Media, Pergamon Press, London, 1960, Section 24*
11. **Froumkine A.** Couche double, electrocapillarite, surtension. In *Actualites Scientifiques et Industrielles, Vol 373, Herman C Editeurs, Paris, 1936, (in French)*
12. **Rastorguev Y. L. and Gantsev Y. A.** Thermal conductivity of liquids in a constant electric field. *Applied Electrical Phenomena*, *1967*, *64–72*
13. **Savinykh B. V., D'yakonov V. G. and Usmanov A. G.** Effect of variable electric fields on the thermal conductivity of dielectric liquids. *J. Eng. Phys.*, *1981*, **41**(*2*), *870–875*
14. **Cheng K. J.** Electric field effects on nucleation during phase transitions of a dielectric fluid. *Phys. Lett.*, *1984*, **106A**, *403–404*
15. **Cheng K. J. and Chaddock J. B.** Effect of an electric field on bubble growth rate. *Int. Commun. Heat Mass Transfer*, *1985*, **12**(*3*), *259–268*
16. **Fritz W.** Berchnung des Maximalvolumens von Dampfblasen. *Phys. Z.*, *1935*, **36**, *379–384* (*in German*)
17. **Choi H. Y.** Electrohydrodynamic boiling heat transfer. *PhD Thesis, Dept. Mech. Eng., MIT, 1962*
18. **Taylor G. I.** Disintegration of water drops in an electric field. *Proc. R. Soc. London A*, *1964*, **280**, *383–397*
19. **Miksis M. J.** Shape of a drop in an electric field. *Phys. Fluids*, *1981*, **24**(*11*), *1967*
20. **Garton C. G. and Krasuchi Z.** Bubbles in insulating liquids: stability in an electric field. *Proc. R. Soc. London A*, *1964*, **280**, *211–226*
21. **Cheng K. J. and Chaddock J. B.** Deformation and stability of drops and bubbles in an electric field. *Phys. Lett.*, *1984*, **106A**, *51–53*
22. **Bergles A. E., Bakhru N. and Shires J. W. Jr** Cooling of high-power-density computer components. *Technical Report No. 70712–60, Heat Transfer Laboratory, Department of Mechanical Engineering, MIT, 1968*
23. **Han C. Y. and Griffith P.** The mechanism of heat transfer in nucleate pool boiling. *Int. J. Heat Mass Transfer*, *1965*, **8**, *887–904*